# *Shroom3* contributes to the maintenance of the glomerular filtration barrier integrity

Nan Cher Yeo,[1,2,12] Caitlin C. O'Meara,[1,2,12] Jason A. Bonomo,[3,4] Kerry N. Veth,[5] Ritu Tomar,[6] Michael J. Flister,[1,2] Iain A. Drummond,[6,7] Donald W. Bowden,[4,8] Barry I. Freedman,[4,9] Jozef Lazar,[1,10] Brian A. Link,[5] and Howard J. Jacob[1,2,11]

[1]*Human and Molecular Genetics Center, Medical College of Wisconsin, Milwaukee, Wisconsin 53226, USA;* [2]*Department of Physiology, Medical College of Wisconsin, Milwaukee, Wisconsin 53226, USA;* [3]*Department of Molecular Medicine and Translational Science, Wake Forest School of Medicine, Winston-Salem, North Carolina 27157, USA;* [4]*Center for Genomics and Personalized Medicine Research, Wake Forest School of Medicine, Winston-Salem, North Carolina 27157, USA;* [5]*Department of Cell Biology, Neurobiology and Anatomy, Medical College of Wisconsin, Milwaukee, Wisconsin 53226, USA;* [6]*Nephrology Division, Massachusetts General Hospital, Charlestown, Massachusetts 02129, USA;* [7]*Department of Genetics, Harvard Medical School, Boston, Massachusetts 02115, USA;* [8]*Department of Biochemistry, Wake Forest School of Medicine, Winston-Salem, North Carolina 27157, USA;* [9]*Department of Internal Medicine - Nephrology, Wake Forest School of Medicine, Winston-Salem, North Carolina 27157, USA;* [10]*Department of Dermatology, Medical College of Wisconsin, Milwaukee, Wisconsin 53226, USA;* [11]*Department of Pediatrics, Medical College of Wisconsin, Milwaukee, Wisconsin 53226, USA*

**Genome-wide association studies (GWAS) identify regions of the genome correlated with disease risk but are restricted in their ability to identify the underlying causative mechanism(s). Thus, GWAS are useful "roadmaps" that require functional analysis to establish the genetic and mechanistic structure of a particular locus. Unfortunately, direct functional testing in humans is limited, demonstrating the need for complementary approaches. Here we used an integrated approach combining zebrafish, rat, and human data to interrogate the function of an established GWAS locus (*SHROOM3*) lacking prior functional support for chronic kidney disease (CKD). Congenic mapping and sequence analysis in rats suggested *Shroom3* was a strong positional candidate gene. Transferring a 6.1-Mb region containing the wild-type *Shroom3* gene significantly improved the kidney glomerular function in FHH (fawn-hooded hypertensive) rat. The wild-type *Shroom3* allele, but not the FHH *Shroom3* allele, rescued glomerular defects induced by knockdown of endogenous *shroom3* in zebrafish, suggesting that the FHH *Shroom3* allele is defective and likely contributes to renal injury in the FHH rat. We also show for the first time that variants disrupting the actin-binding domain of *SHROOM3* may cause podocyte effacement and impairment of the glomerular filtration barrier.**

**[Supplemental material is available for this article.]**

Genome-wide association studies (GWAS) have identified many genetic loci associated with common complex diseases; however, discovering the exact genes remains problematic for several reasons (Manolio et al. 2009). Furthermore, these loci collectively explain only a small percentage of disease heritability, indicating the need to identify alternative sources of "missing" heritability (Manolio et al. 2009; Chatterjee et al. 2013). Genomic infrastructure available for animal models provides a powerful complementary tool to GWAS (Aitman et al. 2008; Geurts et al. 2009; Cox and Church 2011; Lewis and Tomlinson 2012; Atanur et al. 2013; Varshney et al. 2013). For example, mapping quantitative trait loci (QTL) in mammals and identifying natural mutations in syntenic regions of animal disease models have provided functional support for human risk loci in multiple diseases (Aitman et al. 2008). The ability to then genetically manipulate these disease models enables a direct approach to establish causation (Geurts et al. 2009; Cox and Church 2011). Chronic kidney disease (CKD) is a major health issue and is highly heritable (Jha et al. 2013); however, the majority of risk loci causing CKD are uncharacterized and a vast amount of CKD heritability remains to be explained. Here, we leveraged integrated physiological genomics approaches in zebrafish, rat, and human combined with biochemical structural assessment to dissect a highly replicated GWAS locus (*SHROOM3*) and its contribution to renal impairment. Based on our study, we propose that similar approaches can be used to assess many of the 44 other uncharacterized human CKD loci and potentially other loci associated with common diseases (Okada et al. 2012; O'Seaghdha and Fox 2012).

Eight GWAS reported association between intronic *SHROOM3* variants and CKD (Supplemental Table 1); yet, its role in renal function and disease was unknown, and establishing a functional link between *SHROOM3* and renal physiology had been difficult due to early postnatal lethality of *Shroom3* knockout in mice (Hildebrand and Soriano 1999). *Shroom3* encodes an actin-binding protein that regulates morphogenesis of epithelial cells (Hildebrand and Soriano 1999), and it is expressed in the kidney. We note that *Shroom3* is located within a QTL previously found to contribute to albuminuria in the FHH (Fawn-Hooded Hypertensive) rat (Shiozawa et al. 2000). Sequence analysis further identified 13 protein-coding

[12]**These authors contributed equally to this work.**
**Corresponding author: jacob@mcw.edu**
Article published online before print. Article, supplemental material, and publication date are at http://www.genome.org/cgi/doi/10.1101/gr.182881.114.

variants in the FHH *Shroom3* gene compared to the wild-type allele, implicating it as a potential candidate gene in the FHH rat model of CKD. In the present study, we investigated the role of *Shroom3* in kidney function by generating a congenic rat in which the wild-type *Shroom3* allele from BN (Brown Norway) rat was introgressed onto the FHH genetic background. We then utilized hypomorphic and tissue-specific disruption of *shroom3* in zebrafish to test the effect of the gene and its allelic variants on kidney function. We demonstrate that the variants disrupting the actin-binding domain of *SHROOM3* may cause podocyte effacement and impairment of the glomerular filtration barrier. This study establishes the first functional link for *SHROOM3* and kidney pathophysiology.

## Results

### Introgression of the BN *Shroom3* gene onto the FHH genetic background improved glomerular function

We generated a congenic rat strain (named FHH.BN14a) in which a BN-derived 14.50- to 21.40-Mbp region of Chromosome 14 encompassing the *Shroom3* gene was introgressed onto the FHH background and compared its renal phenotypes to the parental FHH strain (Supplemental Fig. 1). At 14 wk of age, both homozygous and heterozygous FHH.BN14a congenic animals showed a significantly lower level of albuminuria, a marker of kidney injury, compared to the FHH rats (Fig. 1A). We measured glomerular permeability to albumin (Palb) in isolated glomeruli from all strains as described previously (O'Meara et al. 2012) and found that Palb in both homozygous and heterozygous FHH.BN14a animals were significantly lower than that in the FHH rats (Fig. 1B). Renal histology showed significantly decreased glomerular sclerosis in the congenic animals compared to the FHH rats (Fig. 1C,D). Electron microscopic analyses of the glomerulus revealed fusion of podocyte foot processes in FHH but not in congenic animals at 18 wk of age (Fig. 1E). These data suggest that replacement of this region containing the BN *Shroom3* allele improved glomerular structure and function in the congenic animals.

We identified 13 amino acid variants (12 missense and a single-amino acid duplication) in the FHH *Shroom3* allele compared with BN rat (Fig. 2A). Six of the 13 variants were predicted computationally to be damaging to *Shroom3* function, and several variants localize to conserved functional domains of the

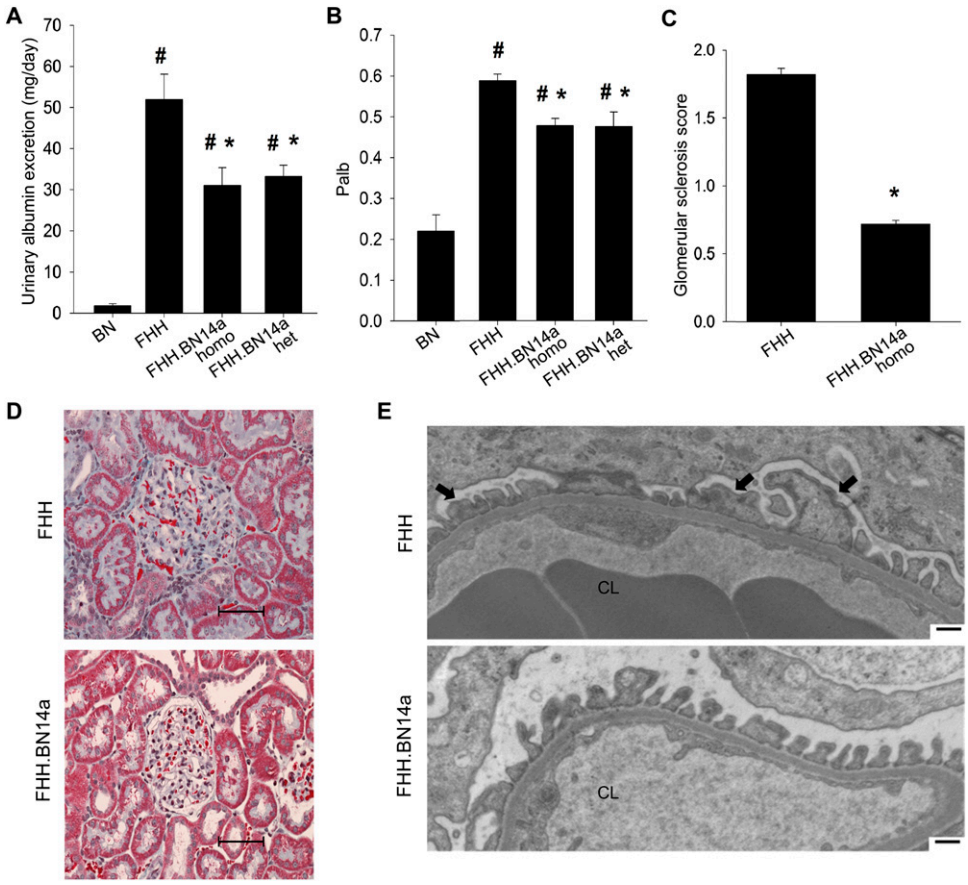


**Figure 1.** Introgression of the BN *Shroom3* gene onto FHH background improves glomerular and overall kidney function. (*A*) At 14 wk of age, both homozygous and heterozygous FHH.BN14a congenic animals showed a significantly lower degree of albuminuria compared to FHH ($n = 4$, 7, 8, and 3, respectively). (*B*) Both heterozygous and homozygous FHH.BN14a demonstrated significantly improved glomerular permeability (Palb) compared to FHH. ($n = 4$ animals/115 glomeruli, 3 animals/76 glomeruli, and 2 animals/70 glomeruli, respectively. Palb in BN was obtained from previously published data [Rangel-Filho et al. 2005].) (*C*) FHH.BN14a kidney showed a decreased presence of glomerular sclerosis compared to FHH at 14 wk of age. A minimum of 30 glomeruli from three kidneys for each strain were scored for a percentage of sclerosis using a scale from 0 (no sclerosis) to 4 (complete sclerosis). (*D*) Representative trichrome-stained images of glomeruli from FHH and FHH.BN14a are shown. Fibrotic tissues are indicated by blue stain. Scale bars = 50 μm. (*E*) Electron microscopic images of glomeruli showed podocyte foot process fusion (indicated by arrow) in FHH compared to FHH.BN14a animals at 18 wk of age. Scale bars = 500 μm. (CL) Capillary lumen, (*) $P < 0.05$ vs. FHH, (#) $P < 0.05$ vs. BN.

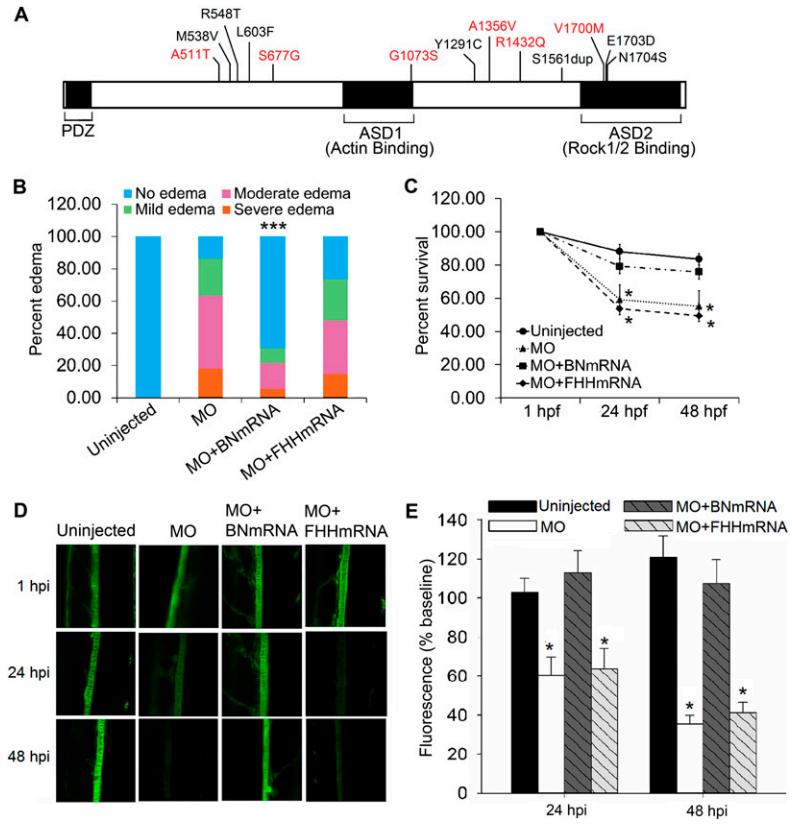


**Figure 2.** FHH *Shroom3* is defective and contributes to glomerular dysfunction. (*A*) Schematic representation of the rat *Shroom3* protein is shown. Vertical lines represent the amino acid variants found in FHH *Shroom3*. Variants predicted to be damaging by PolyPhen-2 are shown in red. (*B*) Co-injection of *shroom3* + *tp53* morpholino (MO) with full-length BN, but not FHH, *Shroom3* mRNA rescued the edema phenotype. ([***] $P < 0.001$ vs. MO and MO + FHHmRNA) and (*C*) cell death induced by *shroom3* + *tp53* MO ([*] $P < 0.05$ vs. uninjected control). (*D*) Representative fluorescence images of individual dorsal aorta at 1, 24, and 48 h following 70-kDa dextran injection are shown. (*E*) Co-injection with BN but not FHH *Shroom3* mRNA rescued the dextran leakage induced by knockdown of endogenous *shroom3* in zebrafish. ($n$ = 35, 26, 23, and 22, respectively. [*] $P < 0.05$ vs. uninjected and MO + BNmRNA.)

protein. Sequence comparison of the entire congenic region identified nine missense variants in addition to those in *Shroom3* (Supplemental Table 2). The only other variants predicted to be damaging were located in genes (*Stbd1* and *Art3*) not expressed in the kidney, making *Shroom3* the most likely candidate responsible for the observed renal phenotypes in the congenic animals.

## FHH *Shroom3* failed to restore glomerular function in zebrafish

In situ hybridization detected *shroom3* expression in the zebrafish pronephric glomerulus and pronephric tubule (Supplemental Fig. 2). We utilized morpholino (MO)-mediated disruption of *shroom3* in zebrafish to assess the impact of *shroom3* on kidney function. We injected one- to four-cell stage zebrafish embryos with a MO antisense oligonucleotide that caused skipping of *shroom3* exon 5 (Supplemental Fig. 3). A MO against *tp53* was co-injected to prevent potential nonspecific cell death (Robu et al. 2007). We observed that uninjected embryos developed normally; whereas *shroom3* + *tp53* MO-injected embryos predominantly (> 85%) displayed cardiac edema (Supplemental Fig. 4A), consistent with pronephros dysfunction (Kramer-Zucker et al. 2005). A fraction of the *shroom3* + *tp53* MO-injected embryos also exhibited gastrulation defects. We analyzed the respective groups using an adaptation of a previously described clearance assay to examine pronephric function (Supplemental Fig. 4B; Hentschel et al. 2007), including knockdown of *cd2ap*, a critical factor for renal glomerular function (Shih et al. 1999), as a positive control in the assay. At 24 and 48 h post-injection (hpi) of 70-kDa fluorescein isothiocyanate (FITC) dextran, we found that the FITC signal was unchanged in the dorsal aorta of uninjected controls and *tp53* MO-alone injected zebrafish (Supplemental Fig. 4C,D). In contrast, zebrafish injected with *cd2ap* + *tp53* MO or *shroom3* + *tp53* MO exhibited significant reduction in FITC signal at 24 and 48 hpi, suggesting that the glomerular size-selective property was compromised after *cd2ap* or *shroom3* knockdown, resulting in an increased rate of clearance of the 70-kDa FITC-dextran (Supplemental Fig. 4C,D).

We next investigated whether co-injection of the zebrafish *shroom3* + *tp53* MO along with *Shroom3* mRNA from either the BN or FHH rats could rescue these defects in zebrafish. Co-injection with BN, but not FHH, *Shroom3* mRNA rescued the pericardial edema and gastrulation defects associated with *shroom3* + *tp53* MO injection (Fig. 2B,C). The glomerular defects induced by knockdown of endogenous *shroom3* were also reversed by BN *Shroom3* mRNA but not the FHH *Shroom3* allele (Fig. 2D,E). These results indicate that the wild-type BN *Shroom3* allele is functional; whereas the FHH *Shroom3* allele is defective and likely contributes to CKD risk in the FHH rat.

## G1073S variant disrupted the actin-binding function of the FHH *Shroom3* allele

A total of 13 protein-coding variants were identified in the FHH *Shroom3* gene, four of which fell in conserved functional domains. We constructed three BN-FHH recombinant *Shroom3* cDNAs, where the BN-specific *Shroom3* sequence was replaced by FHH alleles from nucleotides 641–3044 bp, 3044–4117 bp, or 4117–5966 bp (Fig. 3A). Co-injection of the *shroom3* + *tp53* MO with Shroom3Δ641–3044 or Shroom3Δ4117–5966 mRNA successfully reverted the dextran leakage phenotype observed upon administration of the MO alone; whereas Shroom3Δ3044–4117 mRNA did not, suggesting that at least one of the three variants (G1073S, Y1291C, and A1356V) within this region is damaging (Fig. 3B). We then constructed single-variant substitution alleles (i.e., ΔG1073S, ΔY1291C, and ΔA1356V) and found that the ΔG1073S mRNA failed to rescue glomerular leakage in the zebrafish assay (Fig. 3C,D). The G1073S variant lies in the ASD1 (Apx/Shrm Domain 1) that mediates SHROOM3 interaction with actin (Hildebrand and Soriano 1999), raising the possibility that this aspect of protein function is affected.

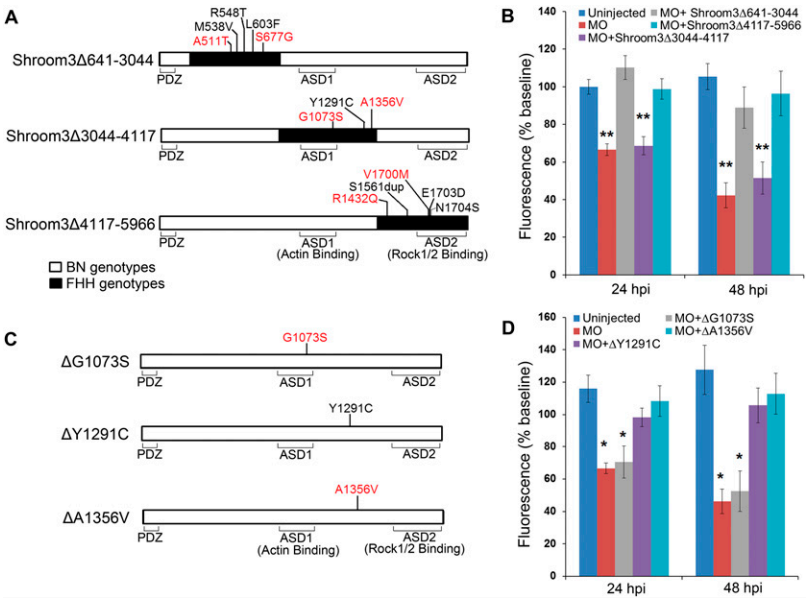


**Figure 3.** The G1073S variant disrupts the function of the FHH *Shroom3* gene. (*A*) Schematic of the different recombinant *Shroom3* cDNAs, where a specific region of the BN *Shroom3* sequence was replaced by FHH. (*B*) Co-injection of *shroom3* + *tp53* MO with Shroom3Δ641–3044 or Shroom3Δ4117–5966 mRNA, but not Shroom3Δ3044–4117 mRNA, rescued dextran leakage induced by the MO ($n$ = 23, 9, 18, 28, and 15, respectively). (*C*) Schematic of *Shroom3* single-amino acid mutants created by site-directed mutagenesis. (*D*) Co-injection of ΔY1291C or ΔA1356V restored normal glomerular permeability, while ΔG1073S failed to exhibit functional rescue ($n$ = 17, 12, 17, 23, and 21, respectively). (*) $P < 0.05$, (**) $P < 0.001$ vs. uninjected.

Coimmunoprecipitation (co-IP) of a Flag-tagged *Shroom3* allele in HEK293 cells demonstrated that the FHH *Shroom3* allele exhibited significantly lower affinity for actin than the BN *Shroom3* allele, and this defect was recapitulated by the ΔG1073S mutant allele (Fig. 4A–C). The *Shroom3* ASD2 domain mediates direct interaction with ROCK proteins (Nishimura and Takeichi 2008), which we examined using the co-IP assay. As expected, mutations in the ASD1 actin-binding domain had no effect on SHROOM3-ROCK1 interaction (Fig. 4A–C). These data demonstrate that the G1073S variant in Shroom3 may disrupt the normal glomerular filtration barrier by compromising the interaction of SHROOM3 with actin.

## P1244L variant disrupted the function of human *SHROOM3* gene

GWAS have detected common noncoding variants in *SHROOM3* that are significantly associated with CKD, but the overall contribution of these variants to CKD risk is modest (Boger and Heid 2011). To identify other potential contributors to the disease risk, we tested variants in the human *SHROOM3* exon5, which harbors the ASD1 actin-binding domain, for association with nondiabetic end-stage kidney disease (ESKD) in 2465 African Americans. The clinical characteristics of the study participants and identification of sequence variants were described in Supplemental Table 3 and Methods. Based on criteria previously described (Bonomo et al. 2014), we selected 20 coding variants and three splice-site variants in the *SHROOM3* exon 5 for genotyping.

Among the coding variants, rs181194611 showed association with ESKD ($P$ = 0.014, OR = 7.95, MAF = 0.0009) (Supplemental Table 4). This rare variant causes an amino acid substitution from a highly conserved proline to leucine at position 1244 (p.P1244L) (Fig. 5A). P1244L lies downstream from the *SHROOM3* ASD1 domain and maps to a homologous region in the mouse ortholog that is known to mediate actin interaction (Hildebrand and Soriano 1999). This variant was predicted to be functionally damaging by PolyPhen-2 (Adzhubei et al. 2010), SIFT (Ng and Henikoff 2001), and PROVEAN (Choi et al. 2012). Co-injection of *shroom3* + *tp53* MO with the nonmutated human *SHROOM3* mRNA restored glomerular function in zebrafish; whereas ΔP1244L mRNA did not (Fig. 5B,C), demonstrating that the P1244L variant indeed impairs *SHROOM3* function and is a damaging mutation that is likely contributing to the underlying pathogenesis of glomerular dysfunction.

To examine the potential role of noncoding variants in *SHROOM3*, we tested 11 *SHROOM3* noncoding variants previously associated with diabetic kidney disease in African Americans (McDonough et al. 2011) and eight noncoding variants located in transcription factor binding sites. Two common intronic SNPs (rs17002091 and rs17002201) previously identified in diabetic kidney disease exhibited association in this study ($P$ = 0.037 and 0.015, respectively, OR = 0.83 for both SNPs) (Supplemental Table 4). No correlation was found between the two SNPs; thus they are likely distinct signals ($r^2$ = 0.004, D′ = 0.286). Analysis of the rs17002091 and rs17002201 haplotypes identified potentially damaging variants (rs72868158 and rs55650799, respectively), which were predicted

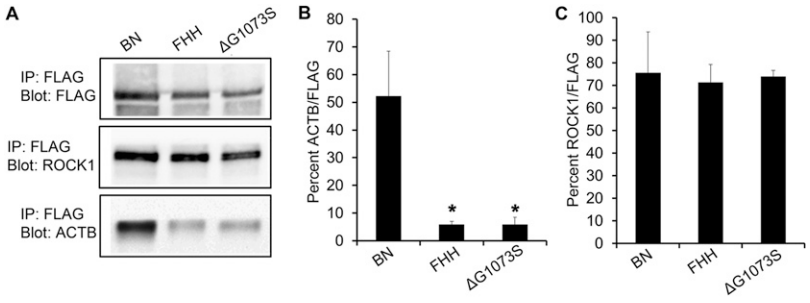


**Figure 4.** The G1073S variant decreases the actin-binding affinity of SHROOM3 protein. (*A*) FLAG-tagged BN, FHH, or ΔG1073S SHROOM3 proteins were overexpressed in HEK293 cells, followed by immunoprecipitation against FLAG. Immunoprecipitated lysates were immunoblotted using antibodies against FLAG, ROCK1, and ACTB. A representative Western blot of immunoprecipitated lysate is provided. (*B*) Quantification of the Western blot showed that FHH SHROOM3 and ΔG1073S mutant had significantly reduced actin-binding affinity compared to BN SHROOM3. ($n$ = 3 per group. [*]$P < 0.05$ vs. BN.) (*C*) ROCK1-binding affinity was not different among the three alleles ($n$ = 3 per group).

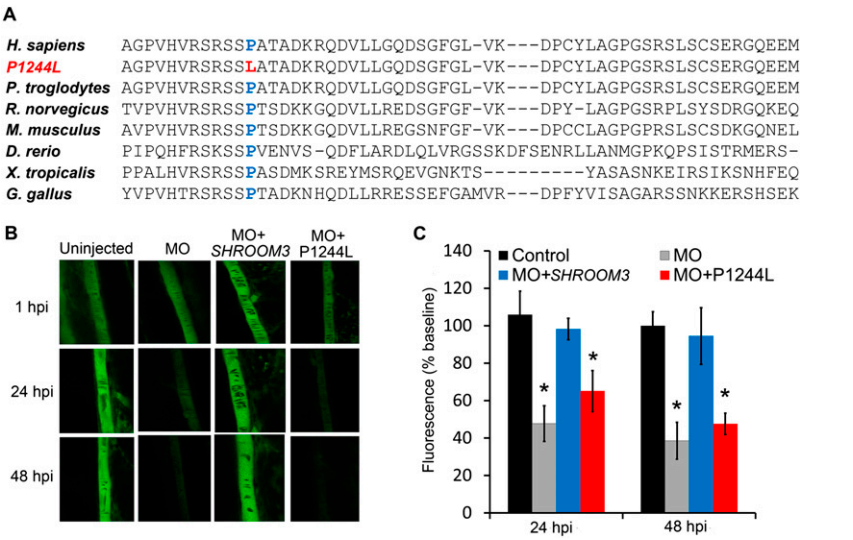


**Figure 5.** rs181194611 (p.P1244L) associated with nondiabetic ESKD impairs *SHROOM3* function in vivo. (*A*) Proline at the amino acid position 1244 in *SHROOM3* is evolutionarily conserved. (*B*) Representative images of dorsal aorta at 1, 24, and 48 h following 70-kDa dextran injection are shown. (*C*) Co-injection of nonmutated human *SHROOM3* mRNA restored normal glomerular permeability, while ΔP1244L failed to show functional rescue. (*) $P < 0.05$ vs. uninjected.

to disrupt transcription factor binding sites by RegulomeDB (http://www.regulomedb.org/) (Boyle et al. 2012). Testing of rs72868158 and rs72663250 (proxy of rs55650799) replicated the association previously observed, suggesting that these\ variants underlie the risk associated at this locus. Our results suggest that both common noncoding variants and rare coding variants affecting *SHROOM3* expression or function may be contributing to the risk of developing complex kidney disease in humans.

### Podocyte-specific disruption of *shroom3* caused podocyte effacement in zebrafish

Injuries targeting the glomerular epithelial cells (podocytes) are a major cause of renal impairment in the FHH rat (Simons et al. 1993; Kriz et al. 1998) and proteinuric kidney diseases in humans (Faul et al. 2007; Brinkkoetter et al. 2013). Considering that *Shroom3* is expressed in the podocytes (Saleem et al. 2008; Brunskill et al. 2011), we hypothesized that it regulates glomerular permeability via its action on podocyte structure. We generated a zebrafish transgenic line carrying a *UAS:shroom3* dominant negative (*shrm3DN*) allele and crossed it with a line expressing GAL4 under the control of the podocyte-specific podocin (*nphs2*) promoter (Supplemental Fig. 5). The *shrm3DN* allele, encoding amino acids 808–1143 of the zebrafish *shroom3*, inhibited endogenous *shroom3* activity (Clark et al. 2012). This knockdown line is a useful tool for dissecting the cell type-specific role of *shroom3* and bypasses the confounding effect of global *shroom3* knockdown. We assessed the glomerular filtration barrier integrity using a dextran clearance assay shown in Figure 6A. Compared to the *podocin:Gal4* control, the *podocin:Gal4;UAS:shrm3DN* animals showed significantly decreased fluorescence at 24 and 48 hpi, indicating impaired glomerular size-selectivity (Fig. 6B,C). Electron microscopic analyses of the pronephric glomerulus revealed podocyte effacement, indicated by a reduced number of podocyte foot processes and increased foot process width (suggestive of podocyte fusion), in *podocin:Gal4;UAS:shrm3DN* animals (Fig. 6D,E). These results imply that *shroom3* is essential for maintaining the glomerular filtration barrier specifically by regulating podocyte integrity.

## Discussion

Mutations targeting the podocyte actin cytoskeleton are the primary cause of many glomerular and proteinuric diseases of the kidney (Faul et al. 2007). The FHH *Shroom3* allele with a defective actin-binding domain failed to maintain glomerular integrity in the zebrafish, while the FHH *Shroom3* construct containing the functional BN-derived ASD1 domain improved overall kidney function in *shroom3*-deficient zebrafish. These data suggest that hypomorphic *SHROOM3* alleles (e.g., FHH and ΔP1244L) with altered actin-binding likely affect the mechanical characteristics of the glomerular podocyte by disrupting normal actin organization or assembly. It is worth noting that at this point, we do not know whether these alleles are truly sufficient or whether a combinatorial effect of alleles within the haplotype might also exert an effect (Flister et al. 2013).

The actin-binding function of *Shroom3* has been shown to be critical for proper morphogenesis of several epithelial tissues (Hildebrand and Soriano 1999; Haigo et al. 2003; Chung et al. 2010; Plageman et al. 2010). For example, *Shroom3* regulates apical constriction in neuroepithelial cells by recruiting existing actin fibers to the apical site of the cell (Hildebrand and Soriano 1999). Depletion of *Shroom3* in the neural plate prevents recruitment of actin, resulting in loss of the apically constricted morphology without affecting the cell polarity (Hildebrand and Soriano 1999). Thereby, it is possible that *Shroom3* regulates the function of kidney podocyte by acting as a morphogenetic regulator. Future studies will be needed to more clearly define the role of *Shroom3* in podocytes and investigate whether *Shroom3* regulates podocyte cytoskeletons through the same mechanisms observed in other epithelial cell types. *Shroom3* interacts with a number of other proteins in addition to actin (Lee et al. 2007; Nishimura and Takeichi 2008). Identification and characterization of these interactions in podocytes will be critical to gain a better understanding of how *Shroom3* affects the glomerular filtration barrier.

Using congenic rats, we showed that a locus containing the *Shroom3* gene modifies the risk of developing renal impairments. The congenic region contains 60 known and 43 predicted genes, some of which may also affect renal phenotypes. Based on sequence data, *Shroom3* appears to be the most likely candidate gene responsible for the renal phenotypes observed in the congenic animals. Transgenic rescue targeting *Shroom3* and then correcting the particular variants identified are logical future studies.

FHH rat is a well-established mammalian genetic model of CKD. This particular strain spontaneously develops proteinuria and glomerular injury associated with podocyte effacement (Kriz et al. 1998). Studies using the FHH rat have led to the discovery of genes including *Shroom3* that may also be important for kidney diseases in human (Lazar et al. 2013; Rangel-Filho et al. 2013). Sequence comparison between the FHH rat and the renal disease-resistant BN rat identified protein-coding variants in genes (*Umod,*

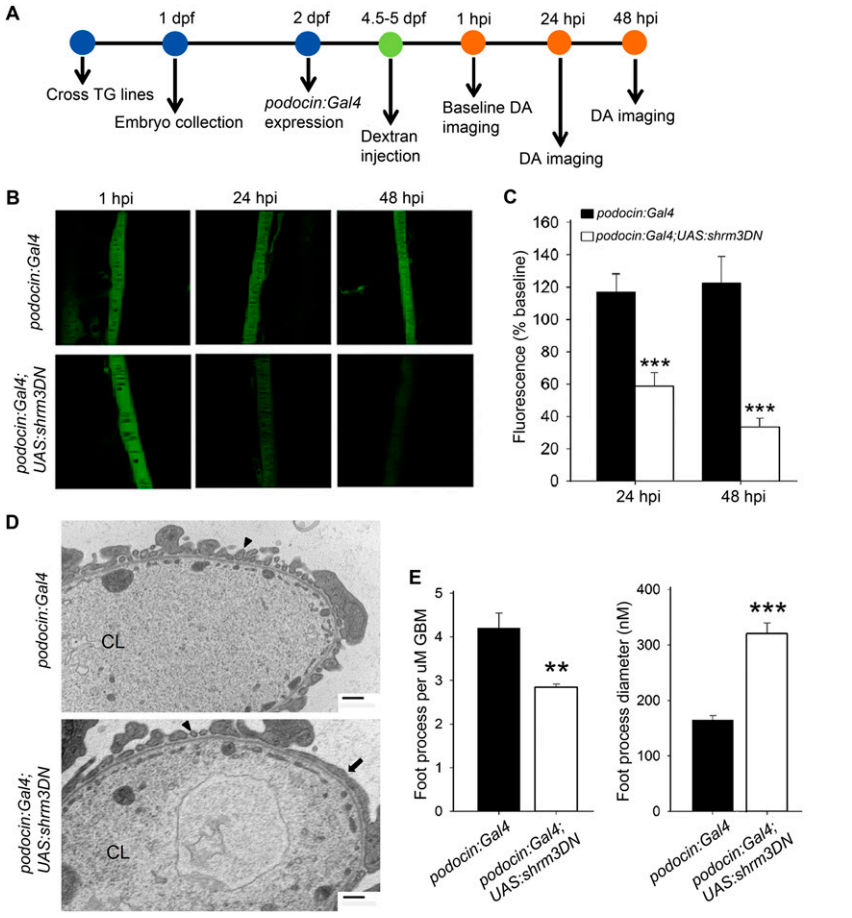


**Figure 6.** Podocyte-specific disruption of *shroom3* causes increased glomerular permeability and podocyte effacement in zebrafish. (*A*) Specific transgenic (TG) lines were crossed to obtain embryos expressing *podocin:Gal4* and *podocin:Gal4;UAS:shrm3DN*. The control and mutants were injected with 70-kDa FITC-labeled dextran at 4.5–5 d post-fertilization (dpf) and analyzed for dextran clearance at 24 and 48 h post-injection (hpi). (DA) Dorsal aorta. (*B*) Representative fluorescence images of individual dorsal aorta at 1, 24, and 48 hpi are shown. (*C*) *podocin:Gal4;UAS:shrm3DN* mutants had significantly decreased FITC signal at 24 and 48 hpi compared to control, indicating that the glomerular filtration barrier was disrupted. ($n = 20$ and 25, respectively. [***] $P < 0.001$.) (*D*) Electron micrograph revealed intact podocyte foot processes (indicated by arrowhead) in *podocin:Gal4* animals. Foot process effacement (indicated by arrow) was observed in the *podocin:Gal4;UAS:shrm3DN* mutants. Scale bars = 500 μm. (CL) Capillary lumen. (*E*) *podocin:Gal4;UAS:shrm3DN* had a significantly reduced number of foot processes contacting glomerular basement membrane (GBM) and increased foot process diameter compared to the control. ($n = 3$ per group. [**] $P = 0.01$, [***] $P = 0.0008$.)

*Alms1, Tfdp2, Dab2, Prkag2, Ino80, Casp9, Mecom, Gnas,* and *Aldh2*), in addition to *Shroom3,* which have been identified by human GWAS for CKD (Supplemental Table 5), making these interesting candidates for future studies.

Human GWAS have identified several intronic variants in the *SHROOM3* gene significantly associated with renal functional traits (Supplemental Table 1); yet, the biological role of the gene/variants has been unclear. The presented studies provide the first functional support for *SHROOM3* contributing to renal diseases in humans rather than just being a genetic marker that is correlated with the disease. Follow-up functional investigations in humans, such as fine mapping of *SHROOM3*, analysis of the gene expression or function associated with the risk haplotype, and case-control studies to test *SHROOM3* and the associated LD region, are necessary. Several lines of evidence have suggested that rare variants can play a role in human complex diseases and could account for a significant portion of the disease heritability (Pritchard 2001; Ji et al. 2008; Zuk et al. 2014). Our association analyses identified a rare variant (P1244L) in *SHROOM3* that impaired the protein function, suggesting that some rare variants in *SHROOM3* may be contributing to renal disease.

In summary, our study shows that *Shroom3* is essential for the maintenance of the glomerular filtration barrier specifically by regulating podocyte integrity. We demonstrate that *Shroom3*-mediated actin interaction is crucial for maintaining normal glomerular function, and mutations within the *Shroom3* actin-associating region may modify the risk for renal impairments. Using a combination of strategies across multiple species and data sets, we demonstrate that a rare variant of *SHROOM3* is unable to rescue renal function in zebrafish, suggesting that it could play a role in the pathogenesis of glomerular impairment in human disease. We also demonstrate that both common noncoding variants and rare coding variants affecting *SHROOM3* expression or function may be contributing to the risk of developing complex kidney disease in humans.

## Methods

### In situ hybridization

Zebrafish *shroom3* cDNA was PCR-amplified using a designed primer pair (Supplemental Table 6) and cloned into the pGEM-T Easy vector (Promega). The plasmid templates were linearized using SacII flanking the 5′-end of *shroom3* sequence. Linearized plasmids were subsequently used for in vitro transcription by SP6 RNA polymerase and DIG RNA labeling mix (Roche) to generate the *shroom3* antisense probe. Whole-mount in situ hybridization was performed as previously described (Thisse and Thisse 2008) on 48-hpf wild-type zebrafish embryos.

### Morpholino and mRNA injections

Morpholino (MO) antisense oligonucleotides were purchased from Gene Tools. The *shroom3* MO was designed to target the intron splice-acceptor site upstream of *shroom3* exon 5. The effect of the *cd2ap* MO was previously reported (Hentschel et al. 2007). A *tp53* MO was co-injected to inhibit potential nonspecific cell death caused upon injection of the experimental MO (Robu et al. 2007). One hundred micromoles of each MO, diluted in Danieu's buffer and 0.1% phenol red, were injected in 9.2 nl per one- to four-cell stage zebrafish embryo. To assess the MO-induced splicing defects, total RNA was extracted from MO-injected or uninjected embryos with TRIzol reagent (Invitrogen), and cDNA was synthesized using the RevertAid First Strand cDNA Synthesis kit (Fermentas). PCR was performed over the splice site to detect alternatively spliced products. The alternatively spliced PCR product was gel-extracted and sequenced. To synthesize the mRNA for the rescue experi-

ments, PCR-amplified full-length BN or FHH *Shroom3* cDNA was cloned into the pGEM-T Easy vector (Promega). Plasmids were linearized by NcoI and in vitro transcribed into mRNA using the mMESSAGE mMACHINE kit (Ambion) according to the manufacturer's instructions. Four hundred picograms of either BN or FHH *Shroom3* mRNA were co-injected along with the MO into one- to four-cell stage embryos. See Supplemental Table 6 for the sequence of MO and PCR primers.

### Zebrafish transgenic lines

The following lines were crossed to make the podocyte-specific *shroom3* dominant negative (shrm3DN) mutant line: Tg(*podocin:Gal4VP16*), and Tg(*dnshroom3:UAS:mCherry,myl7:eGFP*)mw47. To generate the Tg(*podocin:Gal4VP16*) transgenic zebrafish, a 5197-nt fragment of the zebrafish podocin promoter was originally cloned from BAC zC116P9 using forward 5′-TGCTACACCATT AAGGTGACCTGTG-3′ and reverse 5′-TCTGTTGTGAAGTGTCC TCT GGTG-3′ PCR primers. A 3.5-kb subfragment was generated using forward 5′-CGGTCACCGGAAGTTTATAAGTATAT GGG-3′ and reverse 5′-TCTGTTGTGAAGTGTCC TCTGGTGTTT GG-3′ PCR primers and cloned into pENTER 5′-TOPO vector (Invitrogen) and confirmed by sequencing. The final expression construct, pDestTOl2CG2;podocin:Gal4VP16:polyA, was made using the multisite gateway cloning method (Kwan et al. 2007), and transgenics were generated by plasmid co-injection with Tol2 mRNA into one-cell stage zebrafish embryos. Entry clone plasmids for *dnshroom3:UAS:mCherry; myl7:eGFP* were made using Gateway technology (Invitrogen) and Tol2-kit reagents (Kwan et al. 2007). Transgenesis of the Tol2 constructs was achieved by co-injection of transposase mRNA into one-cell stage embryos. Details of the dnshroom3 mode of action and generation of the entry plasmids have been described (Haigo et al. 2003; Lee et al. 2007; Clark et al. 2012). The following primers were used to amplify the dnshroom3 fragment: forward 5′-ATGCGATGTGTAAGTCCTGA-3′ and reverse 5′-TCAACTGTATATAAGCACTT-3′.

### Zebrafish dextran clearance assay

The dextran clearance assay was adapted and modified from a previous study (Hentschel et al. 2007). For the morpholino and mRNA rescue study, 55-h post-fertilization zebrafish were used for injection of the 70-kDa FITC-labeled dextran. Zebrafish 4.5- to 5-d post-fertilization were used for injection of the dextran in the podocyte-specific *shroom3* knockdown study. Experimental zebrafish were anesthetized with tricane and embedded in 1% agarose prior to dextran injections. A total of 9.2 nl of 70-kDa dextran (1 mg/mL) was injected into the zebrafish cardinal vein. Following injection, the dorsal aorta was imaged by confocal microscopy at 1, 24, and 48 h post-injection (hpi). FITC fluorescent intensities were quantified using ImageJ software (National Institutes of Health). The 70-kDa dextran shows a low rate of filtration by an intact glomerulus and therefore should largely remain in circulation. Diminished FITC signal in the circulation at 24 or 48 hpi indicates glomerular leakage.

### Transmission electron microscopy (TEM)

Zebrafish were prepared for TEM imaging as previously described (Soules and Link 2005). Briefly, the blocks were trimmed on a Leica RM2255 microtome, and ultrathin sections were cut and collected on coated grids and stained with uranyl acetate and lead citrate. Montaged images of entire cross-sectioned podocytes were captured on a Hitachi H600 at 8000×. Morphometrics of podocytes, number and size of foot processes, were scored in a masked manner where the individual scoring was unaware of the sample genotype.

### Rat strain sequencing

FHH/Eur/Mcwi and BN/NHsdMcwi genomic DNA was sequenced using an Illumina HiSeq 2000 and analyzed by CASAVA version 1.8.1 (Illumina). All genomic sequences have been deposited in the NCBI BioProject under accession number PRJEB1333 (Atanur et al. 2013). Variants were analyzed by Variant Effect Predictor (http://www.ensembl.org/info/docs/tools /vep/index.html) (McLaren et al. 2010) and PolyPhen-2 (http://genetics.bwh.harvard.edu/pph2/) (Adzhubei et al. 2010).

### Generation of FHH.BNI4a congenic rat and phenotyping for renal function

The FHH-14$^{BN}$/Mcwi consomic strain was initially derived from the FHH/Eur/Mcwi and BN/NHsdMcwi inbred strains using marker-assisted selective breeding (Mattson et al. 2007). The FHH.BN14a congenic rat strain (official name: FHH.BN-[*D14Rat98-D14Hmgc4*]/Hmgc; RGD ID: 8553187) was generated by backcrossing FHH-14$^{BN}$/Mcwi consomic males to FHH/Eur/Mcwi females. Thirteen- to 14-wk-old male rats were phenotyped for 24-h urinary albumin excretion and in vitro glomerular permeability using methods described previously (O'Meara et al. 2012). After urine collection for the albuminuria study, the left kidney of the experimental animals was collected and immediately fixed with 10% buffered formalin for histological analysis. Fixed tissues were stained and analyzed for glomerular sclerotic injury as previously described (O'Meara et al. 2012). For electron microscopic analysis, kidney cortex from 18-wk-old male rats was collected, prepared, and analyzed as previously described (Rangel-Filho et al. 2013). All animals were housed at the Biomedical Resource Center of the Medical College of Wisconsin (MCW) and maintained on Laboratory Rodent Diet 5001 (PMI Nutrition International Inc.) throughout the studies. Experimental protocols were approved by the MCW Institutional Animal Care and Use Committee.

### Cloning of human and rat *Shroom3* plasmids

The full-length BN or FHH rat *Shroom3* cDNA was amplified using PCR and cloned into a pGEM-T Easy vector (Promega) using the manufacturer's protocol. BN-FHH recombinant *Shroom3* plasmids were generated by cloning with restriction enzymes. The pGEM-T Easy vector containing the full-length BN or FHH *Shroom3* cDNA was digested with two enzymes, AgeI and AgrAI, AgrAI and BstEII, or BstEII and NcoI (New England Biolabs). Desired plasmid fragments were gel-extracted and subsequently ligated using T4 ligase (New England Biolabs) to create Shroom3Δ641–3044, Shroom3Δ3044–4117, and Shroom3Δ4117–5966 plasmids (number indicates the base pairs of cDNA replaced by FHH alleles). To create the single amino acid substitution mutant allele, the full-length BN *Shroom3* cloned into the pGEM-T Easy vector was PCR-amplified using Phusion Hot Start II High-Fidelity DNA Polymerase (Thermo Scientific) and phosphorylated primers harboring the mutated sequence. PCR products were subsequently isolated and ligated using T4 ligase. To test the human alleles, we used the commercially available myc-ddk-tagged human *SHROOM3* cDNA ORF (Origene), and the mutant allele was generated using site-directed mutagenesis. See Supplemental Table 6 for the sequence of PCR primers used in this study. All plasmids were sequenced and verified.

### Protein coimmunoprecipitation (Co-IP) assay

Full-length BN *Shroom3*, full-length FHH *Shroom3*, or ΔG1073S mutant cDNA were cloned into the p3xFLAG-CMV-7.1 expression vector (Sigma) and transfected into human embryonic kidney

(HEK) 293 cells using a calcium phosphate transfection method. HEK293 cells were cultured in Dulbecco modified Eagle medium (DMEM) with 10% fetal bovine serum (FBS), 1% L-glutamine, penicillin streptomycin (1×), and sodium pyruvate (1×). At 24 h post-transfection, cells were collected and lysed in lysis buffer (200 mM NaCl, 20 mM Tris, 2 mM EDTA, 1% Triton X-100, and 0.1% SDS) to extract protein. Seven hundred and fifty micrograms of protein was used for immunoprecipitation (IP) against FLAG. IP protein products were separated on 4%–20% Bio-Rad mini-PROTEAN TGX gels and transferred onto PVDF membranes, followed by overnight incubation with primary antibodies against FLAG, ACTB, and ROCK1. Membranes were then incubated for 1 h with horseradish peroxidase-conjugated secondary antibodies and developed with enhanced chemiluminescence reagent (Pierce). Protein bands were visualized using a ChemiDoc XRS+ Imaging System (Bio-Rad). Band intensities were quantified with ImageJ software (National Institutes of Health).

### Antibodies

Primary antibodies used in this study were: mouse anti-Flag (Sigma, F3165), mouse anti-beta-actin (Abcam, ab6276), and mouse anti-Rock1 (Santa Cruz Biotech, sc-17794). Secondary antibodies used were Peroxidase-AffiniPure Donkey Anti-Mouse IgG (Jackson ImmunoResearch Laboratories, 715-035-150).

### Human variant association study

Coding variants in *SHROOM3* exon 5 were identified from 1000 Genomes Project and exome sequencing of an admixed African American population (Bonomo et al. 2014). Coding variants in and near the *SHROOM3* ASD1 domain were selected for genotyping using criteria previously published (Bonomo et al. 2014). Common noncoding variants in *SHROOM3* that showed prior evidence of association (McDonough et al. 2011) and promoter variants predicted to disrupt transcription factor binding by RegulomeDB (http://regulome.stanford.edu/) were also selected for genotyping. Genotyping was performed using the Sequenom MassARRAY platform (Sequenom). Genotype data were analyzed using single SNP association testing as previously described. A *P*-value of 0.05 was used as the threshold to define significance given the a priori of association between *SHROOM3* and measures of renal dysfunction. Details on sample collection, genotyping, and data analyses were previously published (Bonomo et al. 2014). This study was approved by the Institutional Review Board at Wake Forest School of Medicine.

### Statistical analysis

Statistical analyses were performed using Sigma Plot 12.0 software. Data are presented as mean ± SEM. All data were analyzed by either one-way ANOVA followed by the Holm-Sidak multiple comparison test (for multiple groups) or unpaired Student's *t*-test (for two groups). Dextran clearance results obtained from the morpholino-induced knockdown and mRNA rescue failed the normality test; therefore, the data were analyzed by the nonparametric Kruskal-Wallis test followed by the Dunn's multiple comparison. The dextran clearance data obtained from podocyte-specific *Shroom3* mutant at 48 hpi failed the normality test; therefore, data were log-transformed before *t*-test analysis. Zebrafish edema incidence was analyzed by the $\chi^2$ test.

## Data access

The rat sequence variants can be downloaded from the Rat Genome Database in the Genome Browser (http://rgd.mcw.edu/fgb2/gbrowse/rgd_904/) and the Variant Visualizer (http://rgd.mcw.edu/ rgdweb/front/select.html).

## Acknowledgments

We thank M. Hoffman, C. Purman, M. Cliff, A. Buzzell, A. Lemke, J. Wendt-Andrae, and B. Schilling for excellent technical support; C. Wells for help with electron microscopic imaging; and NIH grant support RO1HL069321 (H.J.J.), RO1-DK071041 (I.A.D.), RO1-DK53591 (D.W.B.), RO1-DK070941 (B.I.F.), and RO1-DK071891 (B.I.F.). J.A.B. is supported by F30 DK098836. This project was conceived and directed by H.J.J.

## References

Adzhubei IA, Schmidt S, Peshkin L, Ramensky VE, Gerasimova A, Bork P, Kondrashov AS, Sunyaev SR. 2010. A method and server for predicting damaging missense mutations. *Nat Methods* **7:** 248–249.

Aitman TJ, Critser JK, Cuppen E, Dominiczak A, Fernandez-Suarez XM, Flint J, Gauguier D, Geurts AM, Gould M, Harris PC, et al. 2008. Progress and prospects in rat genetics: a community view. *Nat Genet* **40:** 516–522.

Atanur SS, Diaz AG, Maratou K, Sarkis A, Rotival M, Game L, Tschannen MR, Kaisaki PJ, Otto GW, Ma MC, et al. 2013. Genome sequencing reveals loci under artificial selection that underlie disease phenotypes in the laboratory rat. *Cell* **154:** 691–703.

Boger CA, Heid IM. 2011. Chronic kidney disease: novel insights from genome-wide association studies. *Kidney Blood Press Res* **34:** 225–234.

Bonomo JA, Palmer ND, Hicks PJ, Lea JP, Okusa MD, Langefeld CD, Bowden DW, Freedman BI. 2014. Complement factor H gene associations with end-stage kidney disease in African Americans. *Nephrol Dial Transplant* **29:** 1409–1414.

Boyle AP, Hong EL, Hariharan M, Cheng Y, Schaub MA, Kasowski M, Karczewski KJ, Park J, Hitz BC, Weng S, et al. 2012. Annotation of functional variation in personal genomes using RegulomeDB. *Genome Res* **22:** 1790–1797.

Brinkkoetter PT, Ising C, Benzing T. 2013. The role of the podocyte in albumin filtration. *Nat Rev Nephrol* **9:** 328–336.

Brunskill EW, Georgas K, Rumballe B, Little MH, Potter SS. 2011. Defining the molecular character of the developing and adult kidney podocyte. *PLoS ONE* **6:** e24640.

Chatterjee N, Wheeler B, Sampson J, Hartge P, Chanock SJ, Park JH. 2013. Projecting the performance of risk prediction based on polygenic analyses of genome-wide association studies. *Nat Genet* **45:** 400–405.

Choi Y, Sims GE, Murphy S, Miller JR, Chan AP. 2012. Predicting the functional effect of amino acid substitutions and indels. *PLOS ONE* doi: 10.1371/journal.pone.0046688.

Chung MI, Nascone-Yoder NM, Grover SA, Drysdale TA, Wallingford JB. 2010. Direct activation of Shroom3 transcription by Pitx proteins drives epithelial morphogenesis in the developing gut. *Development* **137:** 1339–1349.

Clark BS, Cui S, Miesfeld JB, Klezovitch O, Vasioukhin V, Link BA. 2012. Loss of Llgl1 in retinal neuroepithelia reveals links between apical domain size, Notch activity and neurogenesis. *Development* **139:** 1599–1610.

Cox RD, Church CD. 2011. Mouse models and the interpretation of human GWAS in type 2 diabetes and obesity. *Dis Model Mech* **4:** 155–164.

Faul C, Asanuma K, Yanagida-Asanuma E, Kim K, Mundel P. 2007. Actin up: regulation of podocyte structure and function by components of the actin cytoskeleton. *Trends Cell Biol* **17:** 428–437.

Flister MJ, Tsaih SW, O'Meara CC, Endres B, Hoffman MJ, Geurts AM, Dwinell MR, Lazar J, Jacob HJ, Moreno C. 2013. Identifying multiple causative genes at a single GWAS locus. *Genome Res* **23:** 1996–2002.

Geurts AM, Cost GJ, Freyvert Y, Zeitler B, Miller JC, Choi VM, Jenkins SS, Wood A, Cui X, Meng X, et al. 2009. Knockout rats via embryo microinjection of zinc-finger nucleases. *Science* **325:** 433.

Haigo SL, Hildebrand JD, Harland RM, Wallingford JB. 2003. Shroom induces apical constriction and is required for hingepoint formation during neural tube closure. *Curr Biol* **13:** 2125–2137.

Hentschel DM, Mengel M, Boehme L, Liebsch F, Albertin C, Bonventre JV, Haller H, Schiffer M. 2007. Rapid screening of glomerular slit diaphragm integrity in larval zebrafish. *Am J Physiol Renal Physiol* **293:** F1746–F1750.

Hildebrand JD, Soriano P. 1999. Shroom, a PDZ domain-containing actin-binding protein, is required for neural tube morphogenesis in mice. *Cell* **99:** 485–497.

Jha V, Garcia-Garcia G, Iseki K, Li Z, Naicker S, Plattner B, Saran R, Wang AY, Yang CW. 2013. Chronic kidney disease: global dimension and perspectives. *Lancet* **382:** 260–272.

Ji W, Foo JN, O'Roak BJ, Zhao H, Larson MG, Simon DB, Newton-Cheh C, State MW, Levy D, Lifton RP. 2008. Rare independent mutations in renal

salt handling genes contribute to blood pressure variation. *Nat Genet* **40:** 592–599.
Kramer-Zucker AG, Wiessner S, Jensen AM, Drummond IA. 2005. Organization of the pronephric filtration apparatus in zebrafish requires Nephrin, Podocin and the FERM domain protein Mosaic eyes. *Dev Biol* **285:** 316–329.
Kriz W, Hosser H, Hahnel B, Simons JL, Provoost AP. 1998. Development of vascular pole-associated glomerulosclerosis in the Fawn-hooded rat. *J Am Soc Nephrol* **9:** 381–396.
Kwan KM, Fujimoto E, Grabher C, Mangum BD, Hardy ME, Campbell DS, Parant JM, Yost HJ, Kanki JP, Chien CB. 2007. The Tol2kit: a multisite gateway-based construction kit for Tol2 transposon transgenesis constructs. *Dev Dyn* **236:** 3088–3099.
Lazar J, O'Meara CC, Sarkis AB, Prisco SZ, Xu H, Fox CS, Chen MH, Broeckel U, Arnett DK, Moreno C, et al. 2013. SORCS1 contributes to the development of renal disease in rats and humans. *Physiol Genomics* **45:** 720–728.
Lee C, Scherr HM, Wallingford JB. 2007. Shroom family proteins regulate γ-tubulin distribution and microtubule architecture during epithelial cell shape change. *Development* **134:** 1431–1441.
Lewis A, Tomlinson I. 2012. Cancer. The utility of mouse models in post-GWAS research. *Science* **338:** 1301–1302.
Manolio TA, Collins FS, Cox NJ, Goldstein DB, Hindorff LA, Hunter DJ, McCarthy MI, Ramos EM, Cardon LR, Chakravarti A, et al. 2009. Finding the missing heritability of complex diseases. *Nature* **461:** 747–753.
Mattson DL, Dwinell MR, Greene AS, Kwitek AE, Roman RJ, Cowley AW Jr, Jacob HJ. 2007. Chromosomal mapping of the genetic basis of hypertension and renal disease in FHH rats. *Am J Physiol Renal Physiol* **293:** F1905–F1914.
McDonough CW, Palmer ND, Hicks PJ, Roh BH, An SS, Cooke JN, Hester JM, Wing MR, Bostrom MA, Rudock ME, et al. 2011. A genome-wide association study for diabetic nephropathy genes in African Americans. *Kidney Int* **79:** 563–572.
McLaren W, Pritchard B, Rios D, Chen Y, Flicek P, Cunningham F. 2010. Deriving the consequences of genomic variants with the Ensembl API and SNP Effect Predictor. *Bioinformatics* **26:** 2069–2070.
Ng PC, Henikoff S. 2001. Predicting deleterious amino acid substitutions *Genome Res* **11:** 863–874.
Nishimura T, Takeichi M. 2008. Shroom3-mediated recruitment of Rho kinases to the apical cell junctions regulates epithelial and neuroepithelial planar remodeling. *Development* **135:** 1493–1502.
Okada Y, Sim X, Go MJ, Wu JY, Gu D, Takeuchi F, Takahashi A, Maeda S, Tsunoda T, Chen P, et al. 2012. Meta-analysis identifies multiple loci associated with kidney function-related traits in east Asian populations. *Nat Genet* **44:** 904–909.
O'Meara CC, Lutz MM, Sarkis AB, Xu H, Kothinti RK, Hoffman M, Moreno C, Tabatabai NM, Lazar J, Roman RJ, et al. 2012. A 4.1-Mb congenic region of Rf-4 contributes to glomerular permeability. *J Am Soc Nephrol* **23:** 825–833.
O'Seaghdha CM, Fox CS. 2012. Genome-wide association studies of chronic kidney disease: what have we learned? *Nat Rev Nephrol* **8:** 89–99.
Plageman TF Jr, Chung MI, Lou M, Smith AN, Hildebrand JD, Wallingford JB, Lang RA. 2010. Pax6-dependent Shroom3 expression regulates apical constriction during lens placode invagination. *Development* **137:** 405–415.
Pritchard JK. 2001. Are rare variants responsible for susceptibility to complex diseases? *Am J Hum Genet* **69:** 124–137.
Rangel-Filho A, Sharma M, Datta YH, Moreno C, Roman RJ, Iwamoto Y, Provoost AP, Lazar J, Jacob HJ. 2005. RF-2 gene modulates proteinuria and albuminuria independently of changes in glomerular permeability in the fawn-hooded hypertensive rat. *J Am Soc Nephrol* **16:** 852–856.
Rangel-Filho A, Lazar J, Moreno C, Geurts A, Jacob HJ. 2013. Rab38 modulates proteinuria in model of hypertension-associated renal disease. *J Am Soc Nephrol* **24:** 283–292.
Robu ME, Larson JD, Nasevicius A, Beiraghi S, Brenner C, Farber SA, Ekker SC. 2007. p53 activation by knockdown technologies. *PLoS Genet* **3:** e78.
Saleem MA, Zavadil J, Bailly M, McGee K, Witherden IR, Pavenstadt H, Hsu H, Sanday J, Satchell SC, Lennon R, et al. 2008. The molecular and functional phenotype of glomerular podocytes reveals key features of contractile smooth muscle cells. *Am J Physiol Renal Physiol* **295:** F959–F970.
Shih NY, Li J, Karpitskii V, Nguyen A, Dustin ML, Kanagawa O, Miner JH, Shaw AS. 1999. Congenital nephrotic syndrome in mice lacking CD2-associated protein. *Science* **286:** 312–315.
Shiozawa M, Provoost AP, van Dokkum RP, Majewski RR, Jacob HJ. 2000. Evidence of gene-gene interactions in the genetic susceptibility to renal impairment after unilateral nephrectomy. *J Am Soc Nephrol* **11:** 2068–2078.
Simons JL, Provoost AP, De Keijzer MH, Anderson S, Rennke HG, Brenner BM. 1993. Pathogenesis of glomerular injury in the fawn-hooded rat: effect of unilateral nephrectomy. *J Am Soc Nephrol* **4:** 1362–1370.
Soules KA, Link BA. 2005. Morphogenesis of the anterior segment in the zebrafish eye. *BMC Dev Biol* **5:** 12.
Thisse C, Thisse B. 2008. High-resolution in situ hybridization to whole-mount zebrafish embryos. *Nat Protoc* **3:** 59–69.
Varshney GK, Lu J, Gildea DE, Huang H, Pei W, Yang Z, Huang SC, Schoenfeld D, Pho NH, Casero D, et al. 2013. A large-scale zebrafish gene knockout resource for the genome-wide study of gene function. *Genome Res* **23:** 727–735.
Zuk O, Schaffner SF, Samocha K, Do R, Hechter E, Kathiresan S, Daly MJ, Neale BM, Sunyaev SR, Lander ES. 2014. Searching for missing heritability: designing rare variant association studies. *Proc Natl Acad Sci* **111:** E455–E464.

*Received August 13, 2014; accepted in revised form September 29, 2014.*